Experimental and model investigations of bleaching and saturation of fluorescence in flow cytometry

Doornbos, R.M.P.; de Grooth, B.G.; Greve, J.

DOI
10.1002/(SICI)1097-0320(19971101)29:3<204::AID-CYTO3>3.0.CO;2-B

Publication date
1997

Published in
Cytometry

 Cytometry 29:204–214 (1997)

Experimental and Model Investigations of Bleaching and Saturation of Fluorescence in Flow Cytometry

Richard M.P. Doornbos,[1] Bart G. de Grooth,[2]* and Jan Greve[2]

[1]Laser Center, Academic Medical Center, Amsterdam, The Netherlands
[2]Applied Optics Group, Faculty of Applied Physics, University of Twente, Enschede, The Netherlands

Received 30 September 1996; Accepted 2 July 1997

We investigated the fluorescence emission from three fluorophores commonly used for labeling cells in flow cytometry. We have demonstrated that the fluorescence emission from cells labeled with fluorescein-isothiocyanate (FITC), phycoerythrin (PE), and allophycocyanin (APC) is considerably saturated and bleached in standard flow cytometric conditions. Therefore, for optimization of fluorescence detection in a flow cytometer, it is important to know the emission kinetics in detail. We made a mathematical model of the optical processes involved: absorption, fluorescence emission, nonradiative decay, photodestruction, and triplet state occupation. The validity of the model was experimentally tested with a set of averaged fluorescence pulses, measured in a large range of intensities and illumination times. The fluorescence of APC could be completely described by the model and produced the following rate constants: photodestruction rate $k_{b1} = 6 \cdot 10^3\ s^{-1}$, triplet state population rate $k_{12} = 2 \cdot 10^5\ s^{-1}$, and depopulation rate $k_{20} = 5 \cdot 10^4\ s^{-1}$. The fluorescence kinetics of FITC- and PE-labeled cells could not be fitted with only three parameters over the entire range, indicating that other optical processes are involved.

We used the model to determine the sensitivity of our flow cytometer and to calculate the optimum conditions for the detection of APC. The results show that in principle a single APC molecule on a cell can be detected in the presence of background, i.e., autofluorescence and Raman scattering by water. Cytometry 29:204–214, 1997. © 1997 Wiley-Liss, Inc.

Key terms: flow cytometry; fluorescein; phycoerythrin; allophycocyanin; photobleaching; photodestruction; triplet state; single molecule detection; quantification

Fluorescence is one of the most sensitive detection techniques. Thus, it is used widely in various fields, e.g., optical microscopy, chromatography, electrophoresis, flow cytometry, and DNA sequencing (9–11,14,16,22,43). The ultimate limit in fluorescence detection, the detection of single molecules, has been achieved by several groups (21,28,34,40).

To optimize fluorescence detection for a certain application, detailed knowledge is required of the optical processes involved. Mathies et al. (19) derived expressions for the steady-state fluorescence emission and the signal-to-noise ratio for a continuously flowing highly diluted B-phycoerythrin solution. They incorporated photobleaching and singlet state saturation, but triplet state influence was neglected.

In flow cytometry, no steady triplet state will generally occur because of the brief excitation of the fluorophores. Therefore, time dependence of the excitation and emission has to be accounted for in a precise calculation, which was shown by Van den Engh and Farmer (37) who reported on photon saturation and bleaching of Hoechst 33258 and propidium iodide fluorescence in flow cytometric measurements. Their experiments indicated a linear dependence of photobleaching on absorbed dose for microsecond excitation pulses. However, photobleaching in biological objects is not yet a well-understood phenomenon (35,38), as was shown recently by Parks et al. (26). They reported the existence of ''fluorescence recovery'' in fluorescein-, phycoerythrin-, and CY5-phycoerythrin-labeled cells, i.e., the reappearance of fluorescence from previously photobleached fluorochromes.

In this article, we focus on optimization of fluorescence detection in flow cytometry. Previous treatments (3–5,12) have mostly optimized illumination intensity and not exploited the emission kinetics of fluorochromes by optimizing intensity and illumination. An exception is the article by Zucker et al. (44), in which a higher fluorescence output was obtained, compared with standard

*Correspondence to: Dr. Bart G. de Grooth, Applied Optics Group, Faculty of Applied Physics, University of Twente, P.O. Box 217, 7500 AE, Enschede, The Netherlands.

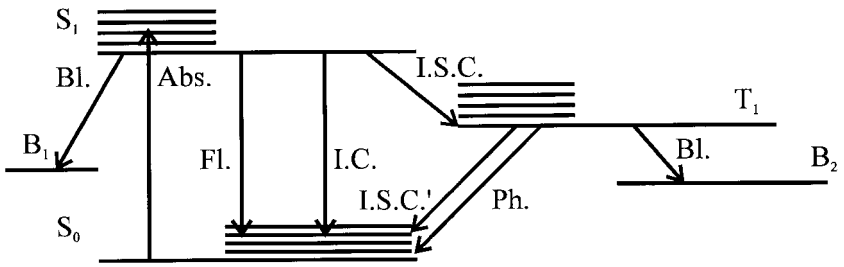

FIG. 1. Jablonski energy diagram of fluorophore. The S and T denote the energy levels of the singlet and triplet states, respectively; B_1 and B_2 represent the energy levels of the bleached molecule; the arrows represent the transitions. Abs., absorption; Fl., fluorescence; I.C., internal conversion; I.S.C., intersystem crossing; Ph., phosphorescence, Bl., bleaching.

instrument performance, when a longer illumination time was introduced by adding tubing to the waste line.

To increase the sensitivity and detection capability of a flow cytometer, we need to find the optimum excitation intensity, flow speed, and fluorophore type for a given experimental problem. To obtain valid estimates, one should take into account the time-dependent excitation and nonlinear effects of fluorescence, such as bleaching and saturation, and the emission from background sources (e.g., Raman scattering of water). For very low signal levels, intrinsic fluorescence of biological cells (autofluorescence) also must be included in the calculations.

We briefly introduce fluorescence and its related processes, which lead to a mathematical description of the kinetics of the molecular system to calculate fluorescence emission for time-dependent excitation. The rate equations describing the fluorescence process can be solved numerically and are implemented in a computer program.

We investigate whether our model can describe experimental data from measurements of fluorescently labeled cells in a flow cytometer. Labeled cells are used to include the environment sensitivity of the fluorophores, so we allow cell-related influences on the fluorescence process. The data set contains series of averaged fluorescence pulse measurements from cells labeled with three commonly used fluorophores: fluorescein-isothiocyanate (FITC), phycoerythrin (PE), and allophycocyanin (APC). Because of the low fluorescence signals obtained when using fluorescently labeled monoclonal antibodies, we used other labeling procedures. We used the Biotin-Streptavidin labeling procedure with APC and PE, and the labeling with FITC was performed using a membrane bound FITC-derivative. We changed both illumination times and illumination intensities to investigate the effects on the fluorescence output. Successful fitting of the model to the experimental data results in values of the rate constants for bleaching and for triplet state population and depopulation.

Once the fluorescence emission can be calculated, it is relatively easy to determine the optimum measuring conditions. The results of the optimization have important implications for the operation and design of the flow cytometer. The possibility of detection of single fluorescent molecules on cells is discussed.

MATERIALS AND METHODS

Theory

Most fluorescent molecules used for labeling and staining in biological applications contain unsaturated carbon bonds. Their electronic structure contains π-orbitals, which are responsible for the fluorescence process (13,25,36). The Jablonski energy diagram of such a molecule is depicted in Figure 1. At room temperature, most molecules are in the electronic singlet ground state, designated by S_0. When a molecule absorbs a quantum of light with sufficient energy, its electronic state is changed very rapidly (in the order of 10^{-15} s) to a particular vibrational level of a singlet state with a higher energy. The vibrational level is left very quickly ($\sim 10^{-12}$ s), and energy is lost by radiationless processes such as collisions with the surrounding molecules and internal conversion (this holds also for the higher electronic levels, which can be neglected here). In general, the molecule will relax to the lowest vibrational level of S_1. From this relatively long living state ($\sim 10^{-8}$ s), the energy can be dissipated in several paths. Emission of a photon (fluorescence) changes the electronic state of the molecule from S_1 to (a vibrational level in) the ground state S_0. This process competes with other de-excitation paths, e.g., solvent relaxation, internal conversion, stimulated emission, chemical reactions, energy transfer processes, and intersystem crossing. In the latter process, the molecule enters the long living triplet state T_1 ($\sim 10^{-3}$ s). From this state, several processes can take place to dissipate energy. One of them, phosphorescence, involves the emission of a photon, but triplet states at room temperature generally decay nonradiatively by solvent collisions, chemical reactions, etc. (13). When during a chemical reaction the fluorescent molecule, either in S_1 or T_1, is changed into a nonfluorescent one, we speak of irreversible bleaching or photodestruction.

The lifetime of a state is given by 1 over the sum of all depopulation rate constants: $\tau = 1/\Sigma k$. The probability of depopulation along a specific route can be expressed by yield constants. For fluorescence, this is defined as the fraction of the rate constant for emission to all rate constants for depopulation of the S_1 state: $Q_f = k_f/\Sigma k$. The radiative or intrinsic lifetime, τ_0, is defined as $1/k_f$.

Model

The kinetics of an ensemble of fluorescent molecules can be described by using population rate equations (38). In these differential equations, the rate by which the system changes from one state to the other is proportional to the population of the initial state. Figure 2 shows our model in which the most important processes are incorporated. We neglect the influence of vibrational levels in each state due to the fast decay.

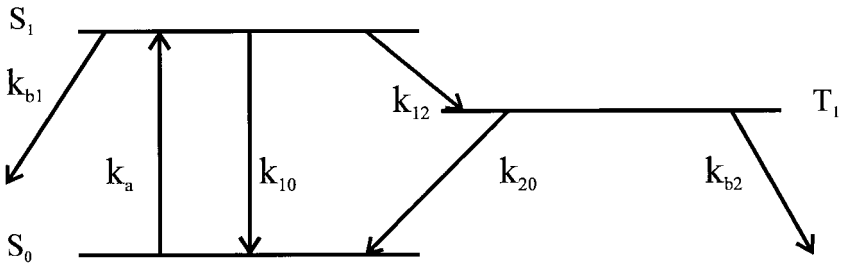

FIG. 2. Diagram of the model used in the program. The S and T denote the singlet and triplet states, respectively, the k's denote the rate constants.

We can write down the following set of coupled first-order differential equations for an ensemble of fluorescent molecules:

$$\frac{dS_0(t)}{dt} = -k_a \cdot S_0(t) + k_{10} \cdot S_1(t) + k_{20} \cdot T_1(t) \quad (1)$$

$$\frac{dS_1(t)}{dt} = k_a \cdot S_0(t) - k_{10} \cdot S_1(t) - k_{12} \cdot S_1(t) - k_{b1} \cdot S_1(t) \quad (2)$$

$$\frac{dT_1(t)}{dt} = k_{12} \cdot S_1(t) - k_{20} \cdot T_1(t) - k_{b2} \cdot T_1(t) \quad (3)$$

where S_0, S_1, T_1 = number of molecules in ground state, excited singlet, and triplet states, respectively; k_a = absorption rate constant, proportional to excitation intensity; k_{10} = depopulation rate constant (fluorescence and internal conversion); k_{12} = rate constant for intersystem crossing from the S_1 state; k_{20} = sum of phosphorescence and intersystem crossing rate from the T_1 state; and k_{b1}, k_{b2} = rates of photodestruction from the S_1 and the T_1 state, respectively.

This set of equations can be integrated to produce the population of each state at time t for given start conditions. The number of molecules is constant and normalized to unity: $S_0(t) + S_1(t) + T_1(t) + N_{bl}(t) = 1$, where $N_{bl}(t)$ is the number of photodestructed molecules. Prior to absorption, all molecules are assumed to be in the ground state. Therefore, we take $S_0(0) = 1$; $S_1(0) = 0$; $T_1(0) = 0$. The fluorescence emission rate can be calculated by multiplying the solution $S_1(t)$ by k_f.

Implementation

The described set of equations can be solved analytically, provided all rate constants are time independent. When one or more rate constants are time dependent, solutions can generally be found only numerically. In our case, k_a is a time-dependent rate constant; therefore, a Pascal program was implemented to solve the set of coupled first-order differential equations. Input to the program are the rate constants and the excitation profile; output is the fluorescence emission intensity profile. The most direct way of solving the equations is using the integration method with a constant step size (Euler method, CS). An improvement to this algorithm with respect to calculation speed is the variation of step size (29). The method using step size variation (SV) is based on a maximum allowed change in the system per integration step: if one step induces changes larger than a specified value, the step size is decreased, and vice versa. For all our SV calculations, we used a maximum allowed change in S_1 of 10^{-5} per step.

Measurements of Saturation and Bleaching of Fluorescently Labeled Cells

Measurements were performed with a home-built flow cytometer and a digital oscilloscope for the recording of pulses. Our flow cytometer consists of a vertically polarized ArKr laser in power-stabilized mode (Coherent Innova 70 Spectrum) using powers of 2–500 mW for 488, 514, and 647 nm. The beam is focused onto a spot by using two cylindrical lenses with focal lengths of 20 and 100 mm. The $1/e^2$-spot diameters are calculated to be approximately 11 μm × 55 μm in the center of the flow cell (Abbott Diagnostics). We used phosphate buffered saline (PBS) with pH 7.2 for sheath flow. The speed of the flow is controlled by an air-pressure regulator in the supply line and flow resistors in the waste line. The use of resistors enables the reduction of the flow speed to values below 0.5 $m \cdot s^{-1}$ (necessary for long illumination times) while pressures remain in the working range of the regulator. Sample delivery is performed by an injection syringe (Hamilton, 100 μl) driven by a stepper motor; this proved necessary for delivery of cells in very slow flows (speeds < 0.5 $m \cdot s^{-1}$).

A gel-immersion objective (NA = 1.2) collects the scattered and fluorescent light in the orthogonal direction and images the light on a diaphragm. The passing light is divided in two parts with a beam splitter; this method ensures identical optical paths for fluorescence and scattered light. Fluorescence (FL) is selected by using band pass filters in combination with long pass filters (to prevent leakage of scattered excitation light). Perpendicularly scattered light (PLS) is reduced in intensity by neutral density filters to prevent saturation of the detector. Both channels are equipped with head-on photomultipliers (Hamamatsu, R1104), which were checked for linearity in the used range because linearity is crucial in these experiments. Forward scattered light between 1° and 3° is detected with a photodiode (PIN 10D, United detector Technology).

Pulses of PLS and FL were recorded on a digital oscilloscope (Le Croy 9360, 8-bit amplitude resolution;

time resolution = 100 Ms·s^{-1} for 1–20 μs/div, down to 10 Ms·s^{-1} for 200 μs/div); each saved pulse shape was an average of 1,000 cell measurements. This was done to remove shot noise and was necessary especially for low-intensity measurements. All pulses were saved in 256-element files on a PC (486DX2, 66 MHz). The oscilloscope was triggered by forward light scattering events.

Cell preparations followed standard protocols: isolated human lymphocytes (PBL) were incubated with octadecylamine-fluorescein isothiocyanate (F18) (15,31) using 150 μl for 4·10^7 cells in 20 ml for 1 h at 37°C. The fluorophores PE and APC were attached in two-step procedures: biotinilation of isolated PBL cells [100 μl NHS-LC-biotin solution (1 μg·ml^{-1}) for 10^7 cells in 1 ml for 1 h at room temperature], followed by incubation with APC or PE conjugated Streptavidin (Becton Dickinson), using 200 μl for 30 min at room temperature. Both incubations were followed by fixation in 1% paraformaldehyde PBS (pH = 7.2). Autofluorescence could be neglected because the cells were strongly labeled.

No special chemical was applied and no special procedure was used to modify bleaching characteristics, such as deoxygenating the media, use of antifading reagents, etc.

Fluorescence lifetime measurements were performed with a time-correlated single photon counting system using picosecond-excitation pulses from a Ti-Saffire laser and a detection system based on a time-to-amplitude converter (23). The solutions of F18 and Streptavidin PE conjugates (pH 7.2) were measured at room temperature.

Fluorescence Pulse Analysis

To obtain a representative set of pulse shapes showing fluorescence saturation and bleaching effects, we measured fluorescence from all fluorophores in a range of intensities and illumination times. For up to four different flow speeds (yielding $1/e^2$ illumination times between 3 μs and 1.2 ms), pulses were measured with various intensities (peak intensities = 5·10^7 to 2.5·10^9 W·m^{-2}). The fluorophores were excited near the absorption maximum: FITC was excited at 488 nm, PE at 514 nm, and APC at 647 nm.

Analysis of the measured pulse shapes can be performed by comparing the FL with the PLS pulse. The first typical effect, saturation, is detected by the flattened appearance of the FL versus the PLS pulse shape and a smaller FL amplitude. The second effect, bleaching, is visible by a smaller FL pulse amplitude and an asymmetric form, and the pulse (peak) appears to be shifted to earlier time, all very dependent on the degree of bleaching.

To quantify these effects, we defined a fluorescence efficiency parameter E by dividing the FL value by the PLS value at each time t (normalized to one at low intensities): E(t) = FL(t)/PLS(t).

This quantity represents the ratio between the emitted fluorescence photon rate and the applied excitation rate, which can be interpreted as fluorescence efficiency. We assume that PLS is proportional to the excitation intensity, which will be verified below. Saturation and bleaching can clearly be recognized in a plot of FL efficiency versus time.

The total influence of an illumination pulse can be expressed by using the parameter *s*, defined by $s = E(t_{after})/E(t_{before})$. This is the ratio of the efficiency after and before illumination, which equals the fraction of molecules that remains available for generating fluorescence after the pulse. Thus, *s* is a measure of the survival of the fluorophore at t_{after}, and the fraction of bleached molecules is $1 - s$. The parameter *s* is not solely a measure of photodestruction; E determined some time after the pulse may be larger than immediately after the pulse, due to, e.g., slow depopulation of the triplet state. However, in case photodestruction is the only process reducing the number of molecules in S_1 ($k_{12} = 0$), the survival parameter *s* can give an estimate of the bleaching rate constant. The subtraction of two values of *s*, determined for different illumination duration divided by the illumination time differences, gives a rough value for the bleaching rate constant k_{b1}.

Fitting of the Fluorescence Model

Fitting the mathematical model to a set of experimental pulses is performed by applying the same rate constants for all used intensities and illumination times and by comparing the measured and calculated FL pulses. The rate constants k_{12}, k_{20}, and k_{b1} are adjusted in a least-squares fitting procedure to obtain the best agreement. We included in our fits only one type of triplet state depletion, so k_{b2} was set to zero.

When significant deviations between results of the model and measurements occur and no good fit can be found, other processes may be involved. In that case, one or more additional transitions or other states may be needed in the model.

To perform quantitative fitting procedures we have made the following assumptions: (1) the measured PLS pulse (averaged over 1,000 cells) is proportional to the excitation intensity profile and can be used for input to the model; (2) the absolute value of excitation intensity in units of photons per square meter is calculated by using the measured laser power, focus diameters, transmission factors, and the fluorescence lifetime; (3) the measured FL pulse (averaged) is proportional to the fluorescence emission; and (4) the absolute value of fluorescence intensity is calculated by using intrinsic lifetime values.

The validity of the first assumption was investigated experimentally. The second and fourth assumptions involve calculations that are shown in the Appendix.

RESULTS

Pulse Shape Analysis

We begin by illustrating the two main nonlinear processes that are included in the model: saturation and bleaching. In Figure 3A, a relatively short illumination of relatively low intensity was used. As can be seen, the measured FL profile follows almost exactly the measured PLS profile. Apparently no saturation and no bleaching have taken place. In Figure 3B, the intensity was chosen 14 times higher. As expected, the PLS pulse was increased 14 times, but the maximum fluorescence intensity was

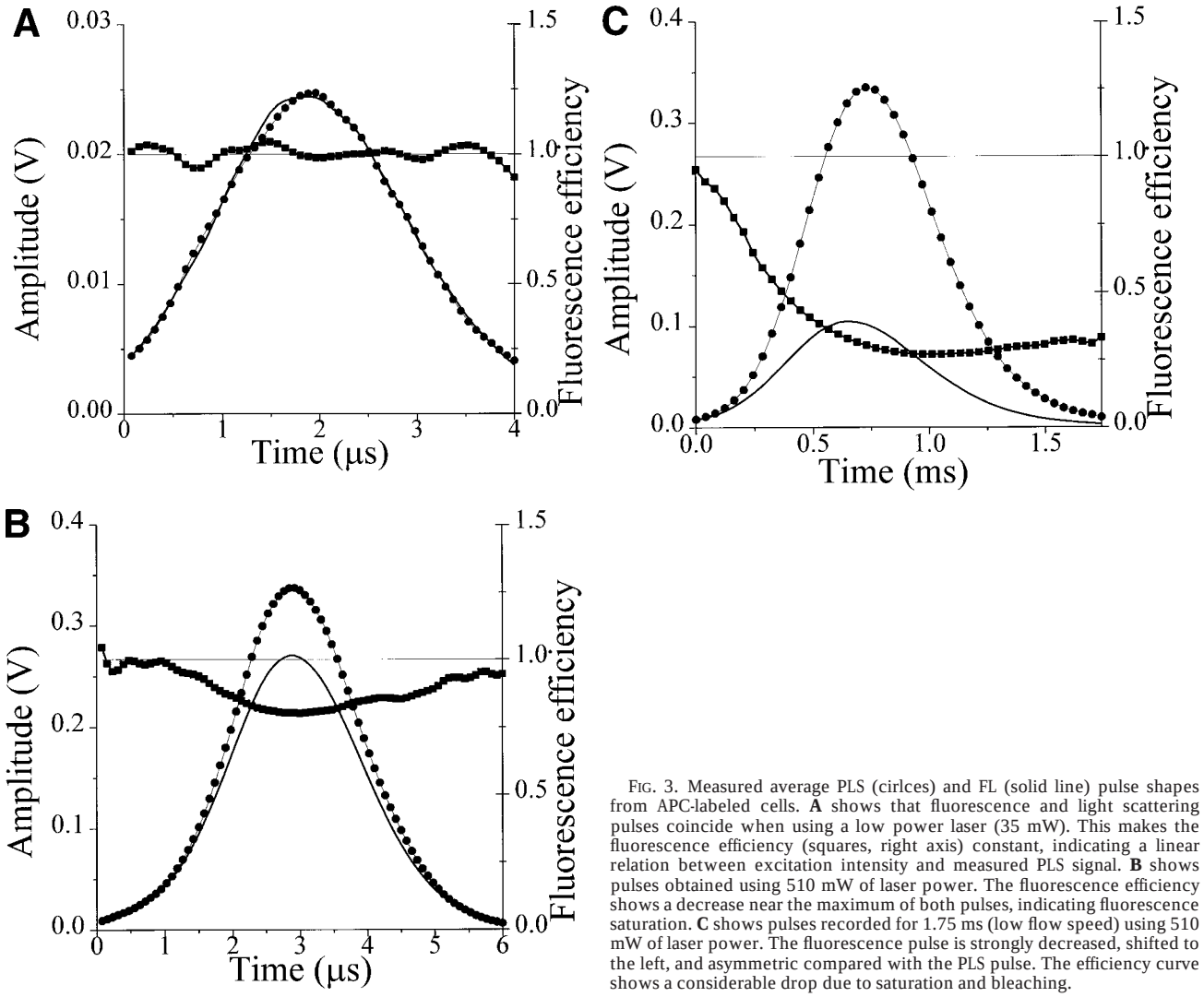

FIG. 3. Measured average PLS (cirlces) and FL (solid line) pulse shapes from APC-labeled cells. **A** shows that fluorescence and light scattering pulses coincide when using a low power laser (35 mW). This makes the fluorescence efficiency (squares, right axis) constant, indicating a linear relation between excitation intensity and measured PLS signal. **B** shows pulses obtained using 510 mW of laser power. The fluorescence efficiency shows a decrease near the maximum of both pulses, indicating fluorescence saturation. **C** shows pulses recorded for 1.75 ms (low flow speed) using 510 mW of laser power. The fluorescence pulse is strongly decreased, shifted to the left, and asymmetric compared with the PLS pulse. The efficiency curve shows a considerable drop due to saturation and bleaching.

only increased 11 times. This result clearly illustrates that saturation occurs under conditions readily achieved in flow cytometry (APC-labeled cells, illuminated with 510 mW of 647-nm light for 4.2 μs in a spot of 11 μm × 55 μm). That the saturation actually takes place during the illumination pulse is clearly seen by the efficiency factor E (= FL/PLS). The fact that this parameter reaches the original value at the end of the illumination period indicates that almost no bleaching has occurred. In Figure 3C, the same high intensity experiment was carried out but at a low flow speed so that an illumination time of 1.2 ms was obtained. It is now clear from the asymmetric fluorescence pulse that, apart from saturation, serious bleaching also occurs. The mentioned nonlinear effects were observed for all fluorophores investigated: FITC, PE, and APC.

We can now answer the question as to whether the PLS pulse shape can be used as an excitation profile in the calculations. From Figure 3A, we see that the fluorescence profile follows the light scattering profile, which proves that the PLS profile is proportional to the excitation profile because fluorescence is linearly dependent on the excitation intensity (for low intensity). Furthermore, the PLS pulse maximum increases linearly with the laser power.

The bleaching effects can be made more explicit, as is shown in Figure 4A, where the survival parameter *s* for APC is plotted as a function of total ($1/e^2$) illumination time. The corresponding curves for FITC and PE are shown in Figures 4b and 4c, respectively. The value of *s* is calculated by using the $E(t_{before})$ value (from the calculations in the Appendix), which is the same for all measurements of each fluorophore, and $E(t_{after})$, which is determined at the time point when the PLS curve reaches $1/e^2$ of the PLS peak height (e.g., in Fig. 3C at 1.4 ms).

For all three fluorophores, the survival decreases with increasing laser power and illumination time, as expected, but it is clear that significant differences in bleaching behavior exist. For FITC and PE, the survival parameter drops very rapidly for short illumination times and then more slowly for longer times. From these figures, it is

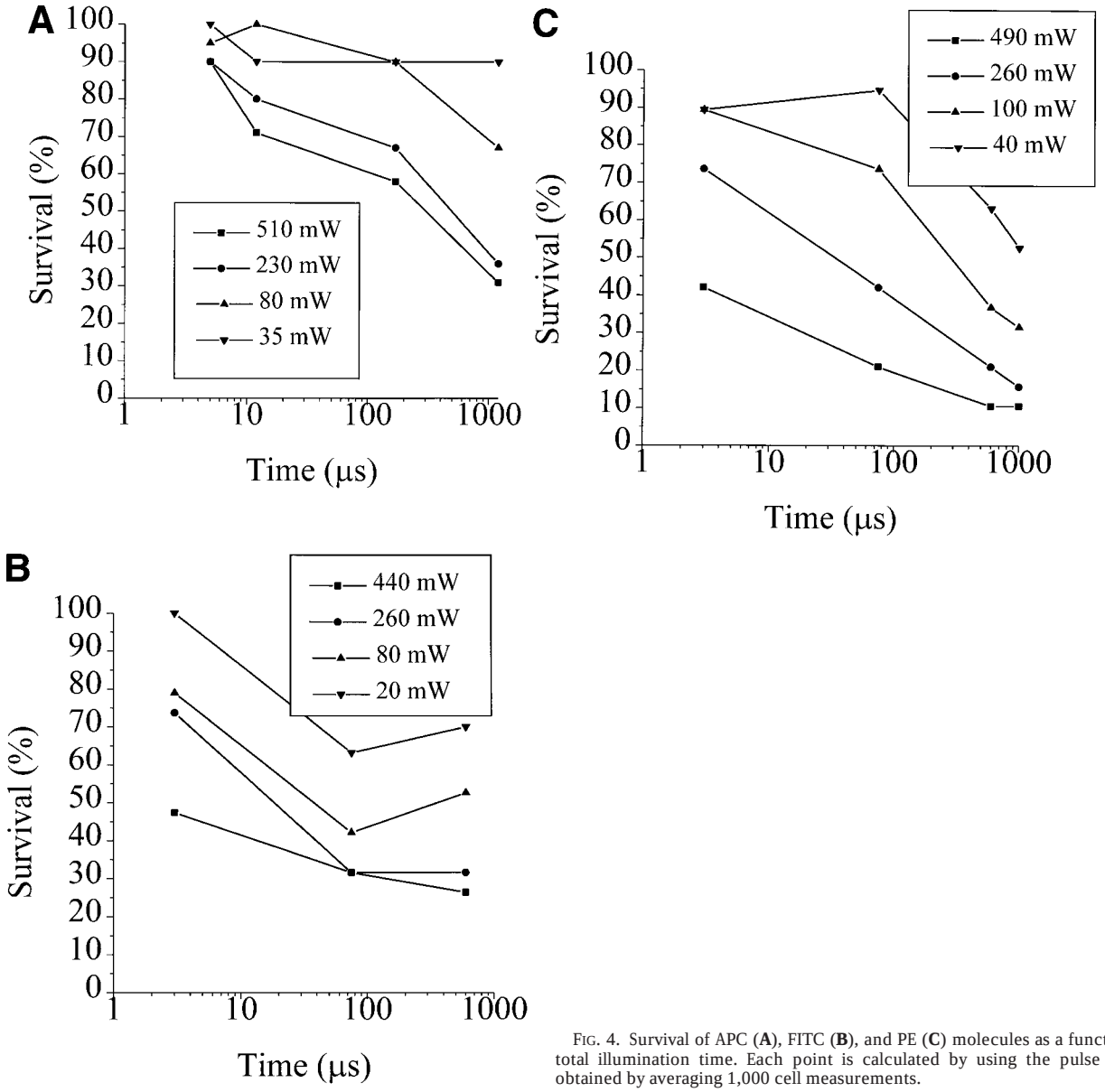

FIG. 4. Survival of APC (**A**), FITC (**B**), and PE (**C**) molecules as a function of total illumination time. Each point is calculated by using the pulse shape obtained by averaging 1,000 cell measurements.

evident that already considerable bleaching occurs for FITC and PE when using microsecond illumination.

Determination of Fluorescence Parameters

To obtain valid input values for the model, we performed lifetime measurements of fluorescent labels. The results are shown in Table 1, where reported values of lifetimes are listed for comparison.

We performed the calculations shown in the Appendix to determine the fluorescence parameters. The resulting values and values reported in the literature of the quantum yields are listed in Table 2. Table 3 lists the extinction coefficients. For APC, the absorption coefficient depends on the concentration due to the dissociation process from trimer to monomer (42).

Table 1
Values of the Measured Lifetime (τ_m) and Lifetimes (τ_{lit}) and Radiative Lifetimes (τ_0) Reported in the Literature[a]

Fluorophore	τ_m (ns)	τ_{lit} (ns)	τ_0 (ns)
FITC	3.7 ± 0.2	3.8 (8), 4.0 (1), 4.4 (20)	6.4 (35)
PE	3.0 ± 0.2	2.1 (20), 3.2 (7)	3.3 (7)
APC	—	2.7 (7), 1.8 (42)	4.0 (7)

[a]Citations to references are given in parentheses.

Calculation Accuracy and Speed

Program checks were performed by comparing the analytical solutions with numerical results by using rectangular pulses. The largest observed differences were approximately 1%. Comparison of the CS and SV calculation

Table 2
Determined Quantum Yields (Q_f) and Quoted Values ($Q_{f,lit}$)[a]

Fluorophore	Q_f	$Q_{f,lit}$
FITC	0.58 ± 0.05	0.50 (27), 0.71 (35)
PE	0.89 ± 0.05	0.98 (7)
APC	—	0.43 (24), 0.68 (7)

[a]Citations to references are given in parentheses.

Table 3
Calculated (ϵ) and Literature (ϵ_{lit}) Values of Extinction Coefficients ϵ[a]

Fluorophore	ϵ (M^{-1} cm^{-1}) (±30%)	ϵ_{lit} (M^{-1} cm^{-1})
FITC	$1.0 \cdot 10^5$	$7.6 \cdot 10^4$ (8), $8.8 \cdot 10^4$ (17)
PE	$3.9 \cdot 10^5$	$1.52 \cdot 10^5$ (7), $1.5 \cdot 10^6$ (39)
APC	$1.1 \cdot 10^5$	$2.3 \cdot 10^4$ (6),[b] $7.0 \cdot 10^5$ (6),[c] $1.31 \cdot 10^5$ (7)

[a]Citations to references are given in parentheses.
[b]Low concentration (monomer).
[c]High concentration (trimer).

methods showed that both methods produced the same results within 1% for steplike excitation profiles. In all tests concerning Gaussian intensity profiles, observed differences were below 0.1%.

The calculation of 1 µs using the CS method (time step 0.1 ns) takes about 1.7 s on a PC (486DX2/66 MHz). On average, the SV method is two to three times faster than the CS method for Gaussian pulse shapes, but this value can be much larger for rectangular pulses. The SV method is definitely the best choice: it is faster than the CS method and has a controllable accuracy.

In flow cytometry, the excitation is time dependent due to the movement of the cell through the laser focus. When we describe the focused laser beam with Gaussian beam optics (41), we obtain a Gaussian time dependence of the excitation intensity. To show the effects of saturation and bleaching on the pulse forms, we show calculated fluorescence pulses in Figure 5. The pulses were calculated with a Gaussian excitation pulse by using peak excitation rates k_a of 0.1 (Fig. 5A), 1 (Fig. 5B), and 10 (Fig. 5C) times the half-saturation value k_{10}. Note that in the low-intensity situation, it is very difficult to distinguish by shape the bleaching effect from the effect of trapping molecules in the triplet state.

Results of Fitting the Model to the Measured Pulses

We have tried to fit simultaneously four pulses representing four times scales from each data set to obtain the rate constants. The measured pulses using high excitation intensities contained the most saturation and bleaching features and were therefore used in the fitting procedures. For APC, one set of rate constants could be found using the model. Table 4 lists the rate constants that give a good fit in the mentioned intensity and time ranges. In Figure 6, we show two examples of the measured and calculated fluorescence emission profiles for APC by using the derived rate constants for a 10-µs (Fig. 6A) and a 1.2-ms (Fig. 6B) illumination time for high intensity.

We have found that, for illumination times shorter than about 100 µs, the fluorescence profile can be described by a model incorporating only photobleaching, which is in agreement with Van den Engh and Farmer (37), but for longer illumination times incorporating the triplet state into the model is essential.

For the data sets of FITC- and PE-labeled cells, we could not find a good fit by using the model, which contains bleaching from singlet or triplet state and occupation and decay of the triplet state (k_{b1}, k_{b2}, k_{12}, $k_{20} \neq 0$). We found that the measured fluorescence pulse form suggests the existence of another process, e.g., the ''fluorescence recovery'' or an oxygen-dependent process.

DISCUSSION

The introduced efficiency (E) and survival (*s*) parameters proved to be very useful in immediate assessment of saturation and bleaching effects. The E parameter shows directly any decrease in fluorescence efficiency, whereas the *s* parameter indicates the total influence of an excitation pulse. The *s* parameter also can be used for a quick estimate of the bleaching rate constant. In experiments requiring real-time bleaching information, these parameters could be computed by using an intelligent oscilloscope.

Pulse shape analysis of our data, as shown in Figure 3, has revealed that fluorescence of FITC- and PE-labeled cells can be severely saturated and bleached in standard flow cytometric conditions (microsecond illumination), whereas for APC only minor saturation could be observed. From Figure 4, it is evident that major differences in emission kinetics exist among FITC, PE, and APC.

The measurements of fluorescence and elastically scattered light may contain small experimental errors. First, the focus size may be too small for a homogeneous illumination of the cells. If that is the case, the emission profile should be described by a convolution of those illumination profile and the fluorochrome density. Second, the polarization of excitation affects the emission of fluorescent labels that are more or less fixed. We assume that the fluorescent dye molecules are reasonably free to rotate within the duration of illumination. For cases in which this is not true, orientational effects have to be considered.

The calculated extinction coefficient of PE is about 25% of the value found by White and Stryer (39). This difference could be caused by the use of a different form of PE or by molecular influences of the lymphocyte environment. Our calculated ϵ value of Streptavidin-bound APC is very close to the value of free APC reported by Grabowski (7). It lies between the values for the monomer and trimer forms, which is plausible because APC at concentrations higher than 10^{-5} M exists as a trimer (42) and tends to dissociate at lower concentrations into three subunits (monomers).

The results of our automated fitting algorithm were interpreted with great care because of the chance of

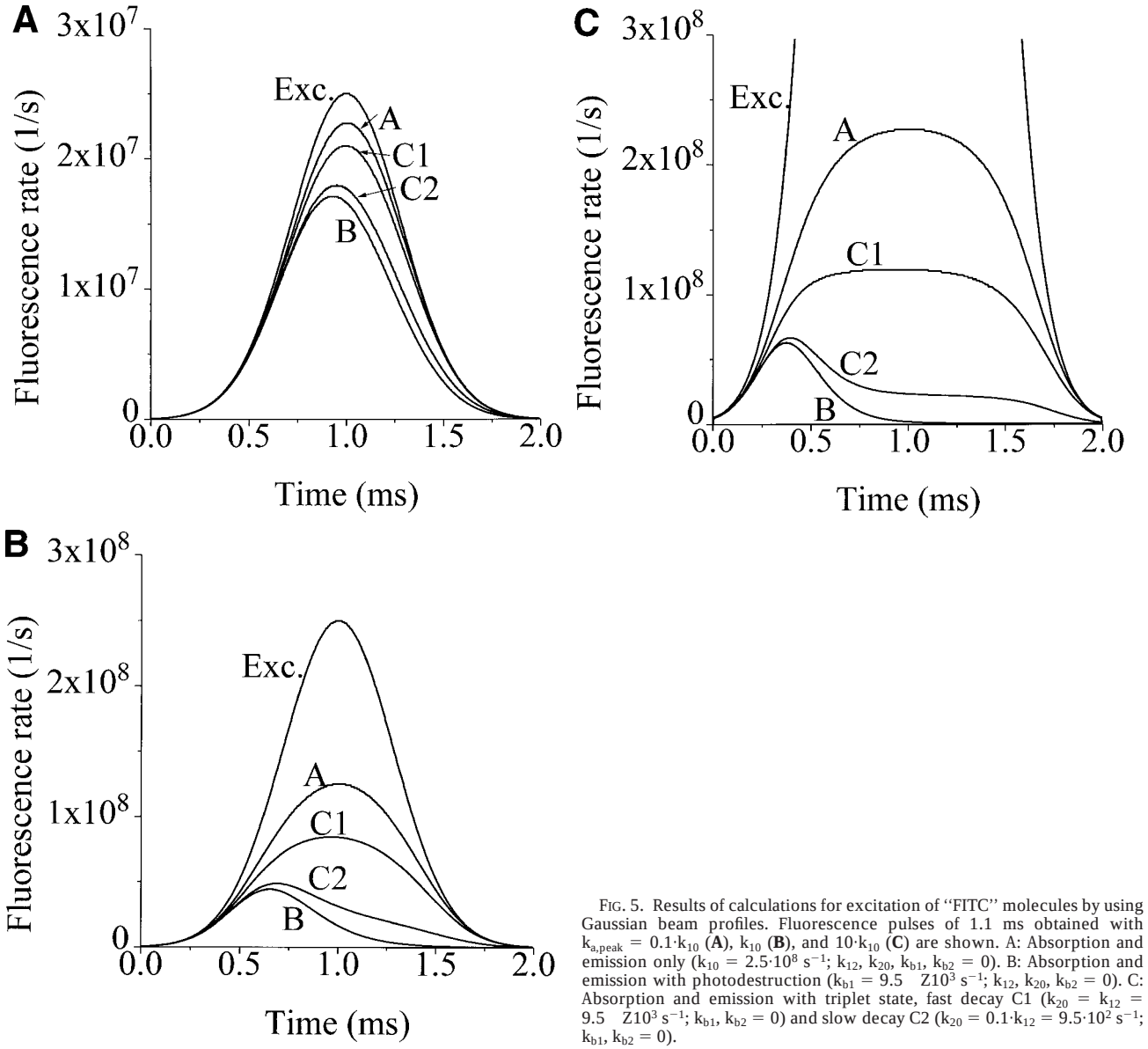

FIG. 5. Results of calculations for excitation of "FITC" molecules by using Gaussian beam profiles. Fluorescence pulses of 1.1 ms obtained with $k_{a,peak} = 0.1 \cdot k_{10}$ (**A**), k_{10} (**B**), and $10 \cdot k_{10}$ (**C**) are shown. A: Absorption and emission only ($k_{10} = 2.5 \cdot 10^8$ s^{-1}; k_{12}, k_{20}, k_{b1}, $k_{b2} = 0$). B: Absorption and emission with photodestruction ($k_{b1} = 9.5$ Z10^3 s^{-1}; k_{12}, k_{20}, $k_{b2} = 0$). C: Absorption and emission with triplet state, fast decay C1 ($k_{20} = k_{12} = 9.5$ Z10^3 s^{-1}; k_{b1}, $k_{b2} = 0$) and slow decay C2 ($k_{20} = 0.1 \cdot k_{12} = 9.5 \cdot 10^2$ s^{-1}; k_{b1}, $k_{b2} = 0$).

Table 4
Results of the Fitting Procedures[a]

Fluorophore	k_{12} (s^{-1})	k_{20} (s^{-1})	k_{b1} (s^{-1})
APC	$2 \cdot 10^5$	$5 \cdot 10^4$	$6 \cdot 10^3$

[a]In the calculations, quantum yield and lifetime values reported by Grabowski (7) are used.

finding suboptima. This effect becomes worse when noisy pulses are involved. Multiparameter fitting proved to be difficult because the importance of a rate constant in the calculation process is dependent on the time scale; its influence is only felt for times equal to or longer than the reciprocal of its value. Therefore, we fitted multiple pulses simultaneously. A practical obstacle for fitting pulses is the long calculation time needed for the simulation of millisecond illumination.

We have shown that the model describes the fluorescence from APC-labeled cells measured by flow cytometry for all used intensities and times, i.e., for intensities below $1.1 \cdot 10^9$ W·m^{-2} and from 5 to 1,200 μs of total illumination time. We estimated the uncertainty in the values of the rate constants to be about 30%. From the bleaching rate constant, the photodestruction quantum yield can be calculated as $1.6 \cdot 10^{-5}$, which is comparable to $4.5 \cdot 10^{-6}$ found for APC solution by White and Stryer (39).

For FITC- and PE-labeled cells, we could obtain a correct description of the fluorescence by using simple bleaching from the excited singlet state but only on microsecond time scales. No set of rate constants could be found that provided a sufficiently good fit for all measured illumination times. This finding raises the question of which other transitions are necessary in the model to describe fully the fluorescence from FITC- and PE-labeled cells. Processes

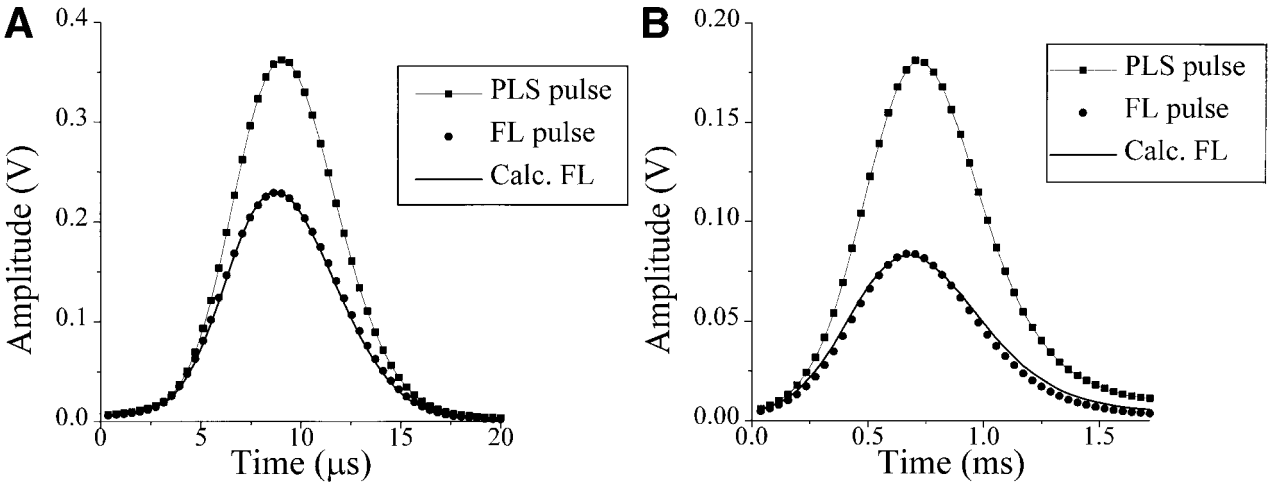

FIG. 6. Comparison of measured and calculated APC fluorescence curves using the model with rate constants determined by fitting. The APC-labeled cells are excited for 10 μs with 510 mW of laser power (**A**) and for 1,200 μs using 230 mW of laser power (**B**).

such as stimulated emission, absorption from excited singlet (26) or triplet state, transitions to intermediate states (17) (oxidized or reduced forms of the fluorophore that can react to all molecules involved), and oxygen-induced quenching or self-quenching may be incorporated in the model. In our case, the most probable candidate is oxygen-induced quenching. Molecular oxygen has a great effect on the bleaching characteristics of fluorescent molecules. Lindqvist (17) showed a strong quenching effect on FITC molecules in the triplet state. In our experiments, oxygen was present, so it is very likely that this process took place. The effect on the measured fluorescence may be complicated by the light-dependent depletion of oxygen and the oxygen diffusion during illumination into the region of the fluorophore. This assumption corresponds with the observation in Figure 4 of the very low survival values for short illumination times.

Application of this method to fluorescent labels conjugated to monoclonal antibodies should in principle produce the same results because the fluorescent molecules are in the same environmental conditions as those in our experiments. The only difference in practice would be the generally lower fluorescent intensities. Therefore, we think our analysis method is widely applicable.

Optimization of Fluorescence Detection in Flow Cytometry: Single Fluorophores?

In designing the most sensitive method of fluorescence detection, the choice of fluorophore is of major importance. This choice must be determined by not only extinction coefficient, quantum yield, fluorescence lifetime, and bleaching characteristics but also the emission spectrum of the fluorophore vs. that of the background sources. From our experiments in recent years (2,30) and those by others (18,32,33,42), we have found that autofluorescence of lymphocytes is the main source of background in flow cytometric measurements using excitation wavelengths up to 550 nm. Above this wavelength, autofluorescence is sufficiently decreased for Raman scattering of water to become the largest background source, depending on the detection volume used. Therefore, in this example, we chose the red-excitable fluorescent label APC to calculate the optimum conditions for the detection of one APC molecule on a lymphocyte. For this molecule, a high extinction coefficient ($7.0 \cdot 10^5$ $M^{-1} \cdot cm^{-1}$) (6), a high quantum yield (0.68) (7), a low bleaching coefficient ($4.5 \cdot 10^{-6}$) (39), and a short fluorescence lifetime (2.7 ns) (7) have been reported. APC is best excited at 650 nm and the emission maximum is approximately 660 nm.

Once the fluorescence emission is calculated using our model, it is relatively easy to find the optimum conditions for detection. The optimum can be found by calculating the signal-to-noise ratio for a range of illumination times and intensities. In the case of using APC and an avalanche photodiode in photon counting mode, we have created a situation in which both autofluorescence and dark current can be neglected; thus, only Raman scattered photons have to be calculated. The results for one APC molecule on a cell (using a detection volume of $11 \times 25 \times 55$ μm^3 and detected fraction of emitted photons $\eta = 0.067$) are shown in Figure 7. For our flow cytometer, the optimum conditions are an illumination time of approximately 1 ms and an intensity of approximately 10^8 $W \cdot m^{-2}$ (corresponding with 30 mW of laser power in our system). We calculated a signal-to-noise value of 15, so true single molecule detection should be possible in these conditions.

In practice, the creation of these optimum excitation conditions may produce some problems. The long illumination time can be obtained by going to low flow speeds, but then the stream becomes very difficult to control, due not only to the high sensitivity to small pressure changes but also to the slow response of the system (in the order of minutes). In addition, at these low speeds, gravity causes cells to sediment, making it impossible to transport the

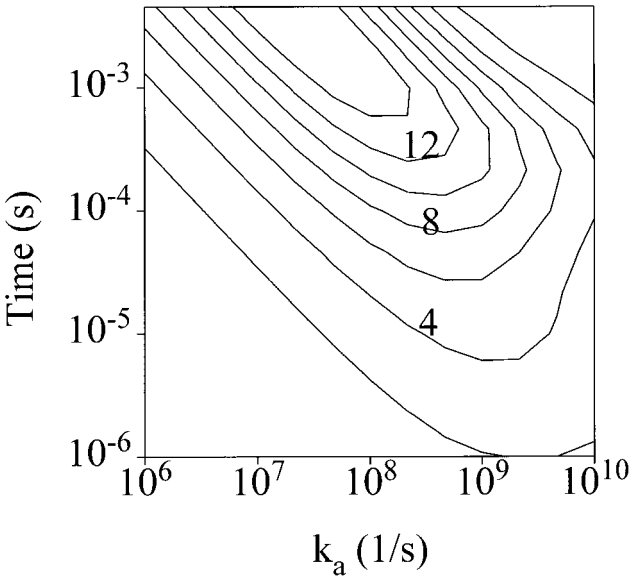

FIG. 7. Results of the signal-to-noise calculation for APC-labeled cells. The signal-to-noise value is plotted as a function of intensity and illumination time in a contour plot.

cells from the sample tube to the flow cell. We found a solution to these problems in flowing vertically by putting a syringe, filled with the cell suspension, directly on top of the flow cell. In this way, gravity acts in the direction of the flow, and stable flows producing millisecond illumination times can be reached. Furthermore, diffusion of the cells to off-axis positions in the flow cell can lead to an inhomogeneously illuminated sample stream. Full solution of these problems may be found in a new design of the flow system.

CONCLUSIONS

Fluorescence from cells labeled with FITC, PE, and APC, as measured with microsecond illumination in a flow cytometer, can be described mathematically by using the fluorescence model. We obtained a good description for APC fluorescence for millisecond illumination times, but a more complex model is required for FITC and PE fluorescence.

Using the fluorescence model and the fluorescence parameters found, we have calculated a signal-to-noise ratio of 15 for optimal excitation conditions of a cell labeled with only one APC molecule.

ACKNOWLEDGMENTS

We thank Loling Song from the University of Leiden, The Netherlands, for helpful discussions on bleaching of fluorescence in biological samples. We also thank Oscar Willemsen, University of Twente, The Netherlands, for performing the lifetime measurements.

LITERATURE CITED

1. Chen RF: Fluorescent protein–dye conjugates. Arch Biochem Biophys 133:263–276, 1969.
2. Doornbos RMP: Optical characterization in flow cytometry: Optimization and miniaturization. Thesis, University of Twente, The Netherlands, 1995.
3. Dusenberry JA, Frankel SL: Increasing the sensitivity of a FACScan flow cytometry to study oceanic picoplankton. Limnol Oceanogr 39:206–209, 1994.
4. Gaucher JC, Grunwald D, Frelat G: Fluorescence reponse and sensitivity determination for ATC 3000 flow cytometer. Cytometry 9:557–565, 1988.
5. Givan AL, Calvert JE, Shenton BK: The effect of improvements in cytometer sensitivity on the detection of CD5-positive B cells with dim fluorescence. Cytometry 12:360–365, 1991.
6. Glazer AN, Stryer L: Phycofluor probes. TIBS 10:423–427, 1984.
7. Grabowski J, Gantt E: Photophysical properties of phycobiliproteins from phycobilisomes: Fluorescence lifetimes, quantum yields, and polarization spectra. Photochem Photobiol 28:39–45, 1978.
8. Haughland RP: Handbook of Fluorescent Probes and Research Chemicals, Ed. 5. Molecular Probes Inc., Eugene, OR, 1992.
9. Hirschfeld T: Optical microscopic observations of single small molecules. Appl Optics 15:2965–2966, 1976.
10. Hirschfeld T: Fluorescence background discrimination by prebleaching. J Histochem Cytochem 27:96–101, 1979.
11. Hirschfeld T: Quantum efficiency independence of the time integrated emission from a fluorescent molecule. Appl Optics 15:3135–3139, 1976.
12. Jett JH, Keller RA, Martin JC, Nguyen DC, Saunders GC: Ultrasensitive molecular-level flow cytometry. In: Flow Cytometry and Sorting, Ed. 2, Melamed MR, Lindmo T, Mendelsohn ML (eds). John Wiley & Sons, New York, 1990, pp 381–396.
13. Jovin TM: Fluorescence polarization and energy transfer: theory and application. In: Flow Cytometry and Sorting, Ed. 1, Melamed MR, Mullaney PF, Mendelsohn ML (eds). John Wiley & Sons, New York, 1979, pp 139–165.
14. Kambara H, Nagai K, Kawamoto K: Photodestruction of fluorophores and optimum conditions for trace DNA detection by automated DNA sequencer. Electrophoresis 13:542–546, 1992.
15. Keller PM, Person S, Snipes W: A fluorescence enhancement assay of cell fusion. J Cell Sci 28:167–177, 1977.
16. Kollner M: How to find the sensitivity limit for DNA sequencing based on laser-induced fluorescence. Appl Optics 32:806–820, 1993.
17. Lindqvist L: A flash photolysis study of fluorescein. Archiv Kemi 16:79–138, 1960.
18. Loken MR, Keij JF, Kelley KA: Comparison of helium–neon and dye lasers for the excitation of allophycocyanin. Cytometry 8:96–100, 1987.
19. Mathies RA, Peck K, Stryer L: Optimization of high-sensitivity fluorescence detection. Anal Chem 62:1786–1791, 1990.
20. Mathies RA, Stryer L: Single-molecule fluorescence detection: A feasibility study using phycoerythrin. In: Applications of Fluorescence in the Biomedical Sciences, Lansing Taylor D (ed.). Alan R Liss, New York, 1986, pp 129–140.
21. Nguyen DC, Keller RA, Jett JH, Martin JC: Detection of single molecules of phycoerythrin in hydrodynamically focused flows by laser-induced fluorescence. Anal Chem 59:2158–2161, 1987.
22. Nishikawa T, Kambara H: Analysis of limiting factors of DNA band separation by a DNA sequencer using fluorescence detection. Electrophoresis 12:623–631, 1991.
23. O'Conner DV, Philips D: Time Correlated Single Photon Counting. Academic Press, London, 1984.
24. Ong LJ, Glazer AN: Crosslinking of allophycocyanin. Physiol Veg 23:777–787, 1985.
25. Parker CA: Photoluminescence of Solutions. Elsevier, Amsterdam, 1968.
26. Parks DR, Bigos M, Moore WA, Herzenberg LA: Short-term and long-term loss of fluorescent dye activity as a function of exposure to laser excitation. Cytometry 6(suppl):85, 1993.
27. Parks DR, Lanier LL, Herzenberg LA: Flow cytometry and fluorescence activated cell sorting (FACS). In: Handbook of Experimental Immunology, Vol. I: Immunochemistry, Weir DM (ed). Blackwell Scientific, Oxford, 1986.
28. Peck K, Stryer L, Glazer AN, Mathies RA: Single-molecule fluorescence detection: Autocorrelation criterion and experimental realization with phycoerythrin. Proc Natl Acad Sci USA 86:4087–4091, 1989.
29. Press WH, Flannery BP, Teukolsky SA, Vetterling WT: Numerical Recipes in Pascal, the Art of Scientific Computing. Cambridge University Press. New York, 1992, p 607.
30. Puppels GJ, Olminkhof JHF, Segers-Nolten GMJ, Otto C, De Mul FFM, Greve J: Laser irradiation and Raman spectroscopy of single living cells and chromosomes: Sample degradation occurs with 514.5 nm but not with 660 nm laser light. Exp Cell Res 195:361–367, 1991.

31. Radosevic K, De Grooth BG, Greve J: Flow cytometric method for simultaneous detection of lymphocyte–K562 conjugates and immunophenotyping of the conjugate forming cells. Cytometry 14:535–540, 1993.
32. Shapiro HM: Multistation multiparameter flow cytometry: A critical review and rationale. Cytometry 3:227, 1983.
33. Shapiro HM: Practical Flow Cytometry, Ed. 3rd. Wiley-Liss, New York, 1995, p 238.
34. Shera EB, Seitzinger NK, Davis LM, Keller RA, Soper SA: Detection of single fluorescent molecules. Chem Phys Lett 174:553–557, 1990.
35. Tsien RY, Waggonner A: Fluorophores for confocal microscopy: photophysics and photochemistry. In: The Handbook of Biological Confocal Microscopy, Pawley J (ed). Plenum Press, New York, 1990, pp 169–178.
36. Turro NJ: Modern Molecular Photochemistry. The Benjamin/Cummings Publishing Co., Menlo Park, CA, 1978.
37. Van den Engh G, Farmer C: Photo-bleaching and photon saturation in flow cytometry. Cytometry 13:669–677, 1992.
38. Wells KS, Sandison DR, Strickler J, Webb WW: Quantitative fluorescence imaging with laser scanning confocal microscopy. In: The Handbook of Biological Confocal Microscopy, Pawley J (ed). IMR Press, 1989, pp 23–35.
39. White JC, Stryer L: Photostability studies of phycobiliprotein fluorescent labels. Anal Biochem 161:442–452, 1987.
40. Wilkerson CW, Goodwin PM, Ambrose WP, Martin JC, Keller RA: Detection and lifetime measurement of single molecules in flowing sample streams by laser-induced fluorescence. Appl Phys Lett 62:2030–2032, 1993.
41. Yariv A: Quantum Electronics. John Wiley & Sons, New York, 1989.
42. Yeh SW, Ong LJ, Clark JH, Glazer AN: Fluorescence properties of allophycocyanin and a crosslinked allophycocyanin trimer. Cytometry 8:91–95, 1987.
43. Zhang JZ, Chen DY, Wu S, Harke HR, Dovichi NJ: High-sensitivity laser-induced fluorescence detection for capillary electrophoresis. Clin Chem 37:1492–1996, 1991.
44. Zucker RM, Elstein KH, Gershey EL, Massaro EJ: Increasing sensitivity of the Ortho analytical cytofluorograph by modifying the fluid system. Cytometry 11:848–851, 1990.

APPENDIX

CALCULATION OF THE ABSOLUTE VALUE OF EXCITATION AND FLUORESCENCE INTENSITY

In this calculation, we use the fluorescence model without bleaching and triplet state occupation ($k_{12} = 0$ and $k_{b1} = 0$). We checked the validity of this model for each fluorophore at short illumination times. The fluorescence emission rate is:

$$F = Q_f \cdot k_{10} \cdot \frac{k_a}{k_a + k_{10}} [ph \cdot s^{-1}],$$

where Q_f is the fluorescence quantum yield, k_a the absorption rate constant, and k_{10} the total decay rate, equal to the reciprocal value of the lifetime: τ^{-1}. Using $k_a = \alpha \cdot V_{PLS}$ and $V_{FL} = \beta \cdot F$, where V_{PLS} and V_{FL} are the voltages of the perpendicular light scattering and fluorescence detector, respectively, and α and β are proportionality factors, it follows that

$$\frac{V_{pls}}{V_{fl}} = \frac{1}{\beta \cdot Q_f \cdot k_{10}} \cdot V_{pls} + \frac{1}{\alpha \cdot \beta \cdot Q_f}$$

The slope and the offset of the V_{PLS}/V_{FL} vs. V_{PLS} graph can be determined by using either pulse peak values (when no bleaching occurs) or that part of individual pulses before bleaching occurs. The lifetime values are obtained by experiment (FITC, PE) or from the literature (APC). This allows calculation of $\beta \cdot Q_f$ and α.

The fluorescence quantum yield can be calculated directly by using the radiative lifetime τ_0: $Q_f = \tau/\tau_0$. The extinction coefficient ϵ can be determined in the following way. By definition, $k_a = \sigma \cdot \Phi$, where Φ is the photon flux, σ is the absorption cross section, and $\sigma = 3.82 \cdot 10^{-25} \cdot \epsilon (m^2)$ (33). The maximum photon flux in focus can be calculated by using $\Phi_{peak} = [(I_{peak} \cdot \lambda)/(h \cdot c)](ph \cdot m^{-2} \cdot s^{-1})$, with $I_{peak} = [(2 \cdot T \cdot P_{total})/(\pi \cdot w_{(e^{-2})x} \cdot w_{(e^{-2})y})](W \cdot m^{-2})$, where I_{peak} is the peak intensity; T is the total transmission factor of lenses and part of the flow cell; P_{total} is the laser power; $w_{(e^{-2})x}$ and $w_{(e^{-2})y}$ are the radii of the focus in both directions; λ is the wavelength; h is the Planck constant; and c is the speed of light. When we take $V_{PLS,peak} = g \cdot P_{total}$, the factor g can be determined by the slope of the graph $V_{PLS,peak}$ vs. P_{total}. Thus, $\sigma = [(\pi \cdot \alpha \cdot g \cdot h \cdot c \cdot w^2)/(2 \cdot T \cdot \lambda)](m^2)$, and ϵ can be calculated.

The accuracy of the extinction coefficient is determined mainly by the accuracy with which slope and offset of the V_{PLS}/V_{FL} vs. V_{PLS} graph is calculated. Another source of inaccuracy is the calculation of the radius of the focus and the total transmission factor.